Available online at www.sciencedirect.com
SCIENCE DIRECT®
International Journal of Solids and Structures 41 (2004) 6597–6612
INTERNATIONAL JOURNAL OF SOLIDS and STRUCTURES
www.elsevier.com/locate/ijsolstr

Optimum strength distribution for seismic resistant shear buildings

R. Karami Mohammadi [a], M.H. El Naggar [b,*], H. Moghaddam [a]

[a] Department of Civil Engineering, Sharif University of Technology, Tehran, Iran
[b] Department of Civil and Environmental Engineering, University of Western Ontario, 1151, Richmond Street, London, Canada N6A 5B9

Received 5 March 2003; received in revised form 20 August 2003
Available online 17 June 2004

Abstract

Structures with inappropriate distributions of strength and stiffness have performed poorly in recent earthquakes, and most of the observed collapses have been related to some extent to configuration problems or a wrong conceptual design. Shear building models of multi-story structures are considered in this study and are subjected to a group of severe earthquakes. It is shown that the strength distribution patterns suggested by the seismic codes do not lead to a uniform distribution and minimum amount of ductility, drift, and damage. A new pattern is proposed that is a function of the period of the structure and the target ductility. An iterative approach is also developed to determine the design strength (and stiffness) pattern needed to achieve a prescribed ductility (or drift) distribution according to different dynamic characteristics of the structure and earthquake. Utilizing this approach, a performance-based design methodology is introduced. This approach is shown to be efficient in finding the optimum strength and stiffness distribution patterns and can also be used to determine the optimum stiffness distribution within buildings with hysteretic dampers, and thus can be used to devise efficient retrofitting schemes using hysteretic dampers.

Keywords: Multi-degree of freedom systems; Ductility; Drift; Optimum strength and stiffness distribution; Seismic codes; Performance-based design; Hysteretic dampers

1. Introduction

The structural configuration of a structure has an important effect on its seismic performance. Structures with inappropriate distributions of strength and stiffness have performed poorly in recent earthquakes, and most of the observed collapses have been related to some extent to configuration problems or an incorrect conceptual design. A soft story has been observed in many collapsed structures because of their nonsuitable distribution of structural strength and/or stiffness (Fig. 1). Different types of strength and stiffness

* Corresponding author. Tel.: +1-519-661-4219; fax: +1-519-661-3942.
E-mail address: naggar@uwo.ca (M.H. El Naggar).

0020-7683/$ - see front matter © 2004 Elsevier Ltd. All rights reserved.
doi:10.1016/j.ijsolstr.2004.05.012

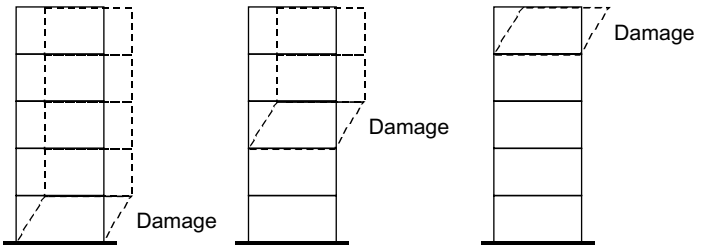

Fig. 1. Various soft stories happened in the collapsed structures.

distribution are responsible for a deficient structural behavior. Concentrated drift and ductility in some stories are the worst type and could result in catastrophic consequences.

The preliminary design of most buildings is based on the equivalent static forces specified by the governing building code. The height-wise distribution of these static forces (and therefore, stiffness and strengths) seems to have been based implicitly on the elastic vibration modes (Green, 1981). However, structures do not remain elastic during severe earthquakes and they usually undergo large nonlinear deformation. Therefore, the employment of such arbitrary height-wise distribution of seismic forces may not necessarily lead to the best seismic performance of a structure.

Chopra (1995) evaluated the ductility demands of several shear building elastoplastic models subjected to the 1940 El Centro Earthquake. The relative story yield strength of these models conformed to the height-wise distribution pattern of the earthquake forces specified in the 1994 Uniform Building Code (UBC). The main finding was that this distribution pattern does not lead to equal ductility demand in all stories, and that in most cases the ductility demands in the first story is the largest among all stories. Moghaddam (1996, 1999) proportioned the relative story yield strength of a number of shear building models in accordance with some arbitrarily chosen distribution patterns as well as the distribution pattern suggested by the UBC. The ductility and displacement demands of these models were calculated. It was concluded that: (a) the pattern suggested by the code does not lead to a uniform distribution of ductility, and (b) a uniform distribution of ductility with a relatively smaller maximum ductility demand can be obtained from other patterns. Consequently, an important question arises: How should the lateral loading pattern in a seismic design procedure of multistory buildings be modified to ensure that the ductility demands are minimal? An objective of this paper is to address this question. An iterative approach has been developed to estimate an optimum loading pattern according to different dynamic characteristics of structure and earthquake.

Many experimental and theoretical studies have focused on hysteretic dampers and buildings with such devices. Most were concerned with the dynamic characteristics of the devices and the behavior of the buildings. There seem to be few studies concerned with the problem of the optimum design of hysteretic dampers and related buildings (Nakashima et al., 1997; Tsuji and Nakamura, 1996; Takewaki et al., 2000; Uetani et al., 2001). In the present paper, the effect of different structural and earthquake characteristics on the optimum distribution of story stiffness of planar shear buildings with hysteretic dampers will be investigated. In this case, the distribution of the maximum inter-story drifts due to earthquakes would coincide with a specified distribution.

2. Modelling and assumptions

Many structural models are used to estimate the nonlinear seismic response of building frames. The shear beam is the most frequently adopted model despite its drawbacks. Shear beam models are widely

used to study the seismic response of multistory buildings because of their simplicity and their low computational requirements, thus permitting the performance of a wide range of parametric studies (Diaz et al., 1994). Lai et al. (1992) have investigated the reliability and accuracy of such shear beam models.

The shear beam models of 5, 10 and 15 story structures with identical story heights have been used in the present study. In these models, each floor is considered as a lumped mass that is connected by perfect elastoplastic shear springs. The total mass of the structure is distributed uniformly over its height. The damping matrix is defined as a linear combination of the mass and initial stiffness matrices resulting in 5% damping for the first few effective modes. In all MDOF models, lateral stiffness is assumed to be proportional to the shear strength at each story, which is obtained in accordance with the selected lateral loading pattern.

The structural models are subjected to seismic excitations and time-history nonlinear dynamic analyses are conducted utilizing the computer program DRAIN-2DX (Prakash et al., 1992), which uses the direct numerical integration method for solving the equations of motion. For each accelerogram, the dynamic response of models with various periods is calculated. Twenty-one accelerograms recorded in 10 different earthquake events are used as the input excitation. Emphasis is placed on those recorded at a low to moderate distance from the epicenter (less than 45 km), with rather high local magnitudes (i.e., $M_L > 6.5$). Since all these records demonstrated high intensities, they represent severe earthquakes and thus are used directly without amplification.

2.1. Lateral loading patterns

In most seismic building codes (Uniform Building Code, 1997; NEHRP Recommended Provisions, 1994; ATC-3-06 Report, 1978; ANSI-ASCE 7-95, 1996; Iranian Seismic Code, 1999), the height wise distribution of lateral forces is determined from the following typical relationship:

$$F_i = \frac{w_i h_i^k}{\sum_{j=1}^{N} w_j h_j^k} \cdot V, \tag{1}$$

where w_i and h_i are the weight and height of the ith floor above the base, respectively; N is the number of stories; and k is the power that differs from one seismic code to another. In some provisions such as NEHRP-94 and ANSI/ASCE 7-95, k increases from 1 to 2 as the period varies from 0.5 to 2.5 s. In some codes such as UBC-97, the force at the top floor (or roof) computed from Eq. (1) is increased by adding an additional force $F_t = 0.07TV$ for a fundamental period T of greater than 0.7 s. In such a case, the base shear V in Eq. (1) is replaced by $(V - F_t)$.

In this study, various loading patterns are obtained by using different values of k in Eq. (1):

$$\begin{cases} 1: k = 0 & \text{: Rectangular loading pattern} \\ 2: 0 < k < 1 & \text{: Rectangular–triangular loading} \quad k = 0.5 + 0.2T \\ 3: k = 1 & \text{: Triangular loading pattern} \\ 4: k > 1 & \text{: } \begin{cases} \text{Parabolic loading pattern} \quad \text{No: 1} \quad k = 1 + 0.4T \\ \text{Parabolic loading pattern} \quad \text{No: 2} \quad k = 1 + 0.8T \end{cases} \\ 5: k \to \infty & \text{: Concentric loading pattern} \end{cases} \tag{2}$$

In addition to the above patterns, the loading patterns of UBC-97, NEHRP-94 and ASCE 7-95 were also considered.

3. Nonlinear spectra for MDOF systems

The inelastic base shear coefficient C_y is equal to the elastic base shear coefficient C_e divided by a reduction factor of R_μ, i.e. $R_\mu = C_e/C_y$. The following procedure is employed to determine the values of C_ys for different ductility factors and can be applied to MDOF structures designed based on different loading patterns.

1. The elastic response spectra were calculated for all seismic records. This provides elastic base shear coefficient for structures with different periods.
2. Inelastic base shear coefficient corresponding to a target ductility factor (at the most critical story) was estimated by interpolating the nearest points. Subsequently, the analysis was repeated to obtain a closer point. The iteration was continued until acceptable accuracy was achieved. In this case, ±2.5% precision for the target ductility was regarded as sufficient.
3. Finally, for any given accelerograms, nonlinear spectra can be constructed by plotting inelastic base shear coefficient, C_y, versus period, T, for various ductility factors.

Utilizing the above procedure, different $C_y - T$ spectra were calculated according to different loading patterns used to design MDOF systems.

4. Adequacy of loading patterns

4.1. Methods to assess the adequacy of a loading pattern

Two main factors should be considered for this purpose: the economy of the seismic resistant system and the extent of the damage. However, it is assumed here that the economy of a seismic resistant system is in proportion to its weight, and that the weight is in turn in proportion to the strength. Consequently, two methods can be used for assessing the adequacy of a loading pattern, namely: (a) the weight-based method, and (b) the damage-based method. These methods are discussed below.

4.1.1. Weight-based method

To evaluate the weight of the seismic resistant system for MDOF structures, it is assumed that the weight of the lateral load-resisting system at each story, W_{Ei}, is proportional to the story shear strength, S_i. Therefore, the total weight of the seismic resistant system, W_E, can be calculated as:

$$W_E = \sum_{i=1}^{n} W_{Ei} = \sum_{i=1}^{n} \lambda \cdot S_i = \lambda \cdot \sum_{i=1}^{n} S_i \tag{3}$$

where λ is the proportioning coefficient.

In an equivalent static force procedure, the normalized vector of loading pattern, Φ_1 defines the lateral seismic forces, $\boldsymbol{F}$:

$$\boldsymbol{F} = \Phi_1 \cdot V \tag{4}$$

where V is the base shear. Then, the shear strength of the ith story can be determined from:

$$s_i = \sum_{j=i}^{n} f_j = \sum_{j=i}^{n} \phi_{1j} \cdot V \tag{5}$$

Therefore, the strength distribution pattern could be represented by Φ_2 where $\phi_{2i} = \sum_{j=i}^{n} \phi_{1j}$. Hence:

$$\boldsymbol{S} = \Phi_2 \cdot V \tag{6}$$

Combining Eqs. (3) and (6), we have:

$$W_E = \lambda \cdot \sum_{i=1}^{n} \phi_{2i} \cdot V = \lambda G V \tag{7}$$

or

$$w = W_E/W = \lambda G C_y \tag{8}$$

where w and W are the relative weight of the seismic resistant system and the total weight of a structure, respectively, and $G = \sum \phi_{2i}$. Parameter GC_y is termed the "weight index" throughout this paper. To determine the most adequate loading pattern we should:

1. Choose a loading pattern and a target ductility ratio, calculate the $C_y - T$ spectrum for the given earthquake as explained in Section 3, and determine the $GC_y - T$ spectrum accordingly. This procedure is repeated to determine the $GC_y - T$ spectra for different ductility ratios.
2. Choose a different loading pattern and repeat step 1 to determine the $GC_y - T$ spectra. We can now compare the weight index GC_y for structures of identical period and ductility ratio that have been designed for different loading patterns, and, therefore, assess the relative adequacy of the chosen loading patterns. The loading pattern that corresponds to the spectrum showing minimum GC_y would be regarded as the most adequate loading pattern.

4.1.2. Damage-based method

It is of interest to compare the seismic behavior of structures of identical total seismic resistance that have been designed according to different seismic loading patterns. Again, it is assumed that for a seismic resistant system, the cost is proportional to the weight and strength. Therefore, it is assumed that the costs of providing seismic resistance for such structures are the same. Consequently, any structure that performs better during an earthquake would represent a better design, and the corresponding loading pattern used for the design of such a structure may be considered more adequate. The ductility ratio has been used here as the criterion for assessing seismic behavior. The procedure to determine the most adequate loading pattern is as follows.

1. A loading pattern is chosen and $G = \sum_{i=1}^{n} \phi_{2i}$ is calculated.
2. An arbitrary value is chosen for the relative weight of the seismic resistant system $w = W_E/W$ Assuming an identical total weight of W for all structures, W_E is determined and substituted in Eq. (7) to obtain the base shear V. The strength distribution is now determined from Eq. (5).
3. The structure is subjected to the given earthquake, and the ductility ratio at the most critical story is evaluated.

These steps are repeated for different seismic loading patterns. Any pattern that leads to the least ductility demand would be regarded as the most adequate.

4.2. Adequacy of loading patterns

Using the methods described above, the adequacy of loading patterns considered in this study has been examined, and more suitable patterns are presented and discussed.

4.2.1. Weight-based method

Fig. 2 illustrates the $GC_y - T$ spectra for 5 and 15 story models with a target ductility ratio of six. These $GC_y - T$ spectra represent the average of the results for all earthquakes considered. The figure shows that

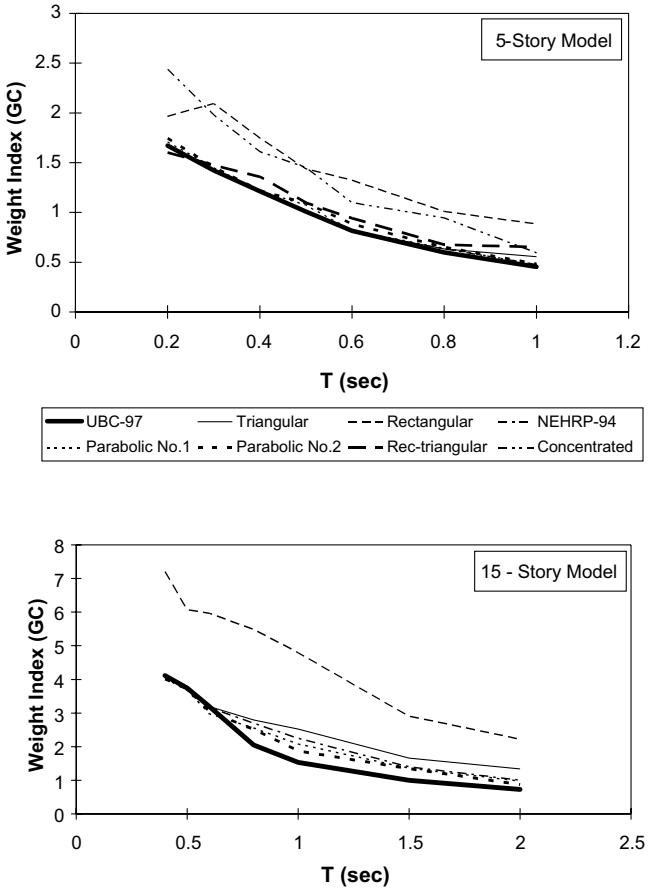

Fig. 2. Weight index *GC* for different loading patterns (used for design of shear building models with a target ductility ratio of 6).

the UBC loading pattern is more suitable compared to all the loading patterns considered for the target ductility ratio of six. This is especially true for structures with lower frequencies.

4.2.2. Damage-based method

Fig. 3 provides the mean $GC_y - \mu$ spectra for 10 story models with a period of 0.8 s. These spectra have been calculated by averaging the results for the 21 earthquakes considered. In a damage-based method, an optimum pattern should result in the least ductility demand on the structure. The results presented in Fig. 3 demonstrate the relative adequacy of different loading patterns.

Karami Mohammadi (2001) introduced an "optimum" loading pattern as a function of the period of the structure and target ductility. The proposed loading pattern is superior to the seismic loading patterns suggested by most seismic codes because, unlike them, it is a function of the target ductility. This loading pattern is a rectangular pattern accompanied by a concentrated force αTV at the top floor, where α is a coefficient that depends on the fundamental period, T, and the target ductility, μ. The following expression is suggested for α to attain an optimum loading pattern:

$$\alpha = (0.9 - 0.04\mu) \cdot e^{-(0.6+0.03\mu)T} \tag{9}$$

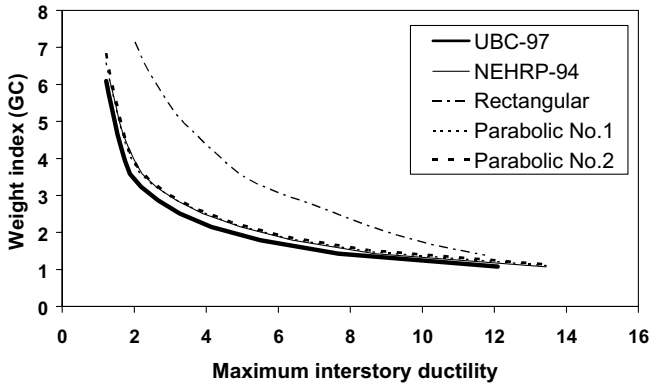

Fig. 3. GC–μ spectra for 10-story buildings designed according to different loading patterns with a period of 0.8 s.

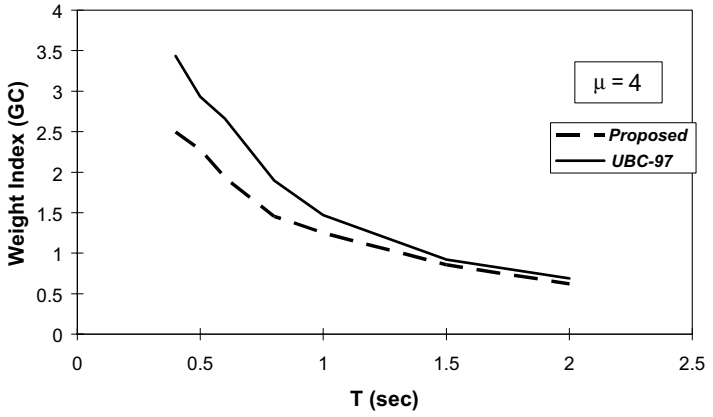

Fig. 4. A comparison of the weight index GC for the proposed and UBC patterns for 10-story building models with target ductility ratio of 4.

In Fig. 4, the $GC_y - T$ spectrum for 10-story models with a ductility ratio of four designed according to the proposed loading pattern is compared with that developed for buildings designed according to the UBC loading pattern.

5. Height wise distribution of ductility demands

Table 1 shows the coefficient of variation (COV) of story ductility demands for 10-story models with a period of 1.0 second that are designed to conform with different strength distribution patterns. These amounts have been obtained by averaging the responses to 21 earthquake records. The design base shear has been adjusted so that to arrive at a maximum target ductility ratio of six in these models. Table 1

Table 1
A comparison of the coefficient of variation of ductility demands for different loading patterns (10-story building with a period of 1.0 s and a target ductility ratio of 6)

Loading pattern	Proposed	UBC 97	Parabolic2	Parabolic1	NEHRP	Triangular	Rectangular
COV	0.295	0.315	0.400	0.439	0.472	0.529	0.865

indicates that the UBC, and the proposed loading patterns have resulted in more uniform distributions of ductility demands relative to other loading patterns. Similar results were obtained for 5 and 15-story models. Therefore, it seems that there exists a close correlation between uniformity of ductility demand distribution and the seismic loading pattern used. Hence, an enhancement in the distribution of ductility demand is accompanied by a better seismic performance. This may be attributed to maximizing the dissipation of the seismic energy in each story, and minimizing the forces imposed on the structure.

6. Optimum patterns for strength distribution

It is known that the seismic response of a structure depends predominantly on the overall distribution of yield strength within the structure. Consequently, the following questions arise: (a) Can we find a particular distribution pattern of yield strength for a structure to achieve the best seismic performance (i.e. the least ductility demand) in a given earthquake? Any given pattern that satisfies this criterion can be regarded as an *optimum* pattern; (b) Would such yield strength distribution pattern be unique? That is, is there just one pattern or multiple patterns that conform to the above requirements?; (c) If there is at least an optimum pattern, how can such a pattern be determined?

Karami Mohammadi (2001) showed that the seismic loading patterns suggested by all codes do not lead to a uniform distribution of ductility, and that a uniform distribution of ductility with the same maximum ductility demands can be obtained from other patterns. Therefore, the objective of this section is to establish a procedure to derive an optimum strength distribution pattern that leads to a uniform distribution of ductility demands, and consequently, an improved seismic performance.

Takewaki (1996, 1997a,b) proposed a method to find a strength (and stiffness) distribution pattern to receive a uniform ductility distribution within the height of structure under a given set of earthquakes. However, the final ductility demand in the proposed method is less than the ductility capacity of each story. Therefore, the proposed strength distribution may not be the optimum.

Karami Mohammadi (2001) proposed an iterative procedure to determine the optimum strength distribution pattern for a structure subjected to a given earthquake. In this procedure, the seismic strength is distributed within the stories according to an arbitrary chosen pattern, such as the pattern shown as step 1 in Fig. 5. The structure is subjected to the given earthquake (the Park Field Earthquake was used in the example considered here). The corresponding normalized ductility demands that are induced to the structure by the end of step 1 are calculated (shown in Fig. 5 as dotted lines). Fig. 5 shows that the smallest ductility demand is located at the fourth story. In step 2, a small decrease is applied to the strength of the

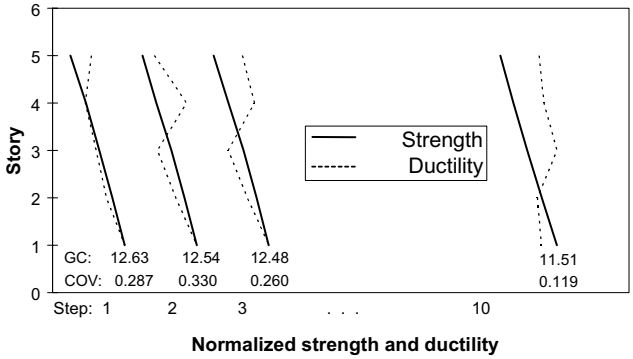

Fig. 5. The iterative procedure to obtain optimum strength distribution pattern for a five-story model with a period of 0.4 s subjected to Parkfield earthquake with a target ductility ratio of 8.

floor with the smallest ductility demand (the fourth floor in this case). This results in an increase in the ductility demand of that story (89% in the given example), accompanied by a decrease in the ductility demands of the other stories. Now, the smallest ductility demand has shifted from the fourth to the fifth story. In step 3, a small reduction of the strength is applied to the fifth story, which results in an increase in its ductility demand (53%). The procedure continues until a rather uniform distribution of ductility demands is obtained at step 10. In this example, the coefficient of variation (COV) of ductilities in step 10 is 0.119, which is approximately 40% of the initial COV in step 1. It is concluded that using the strength distribution in step 10 results in a far better distribution of ductility demands. The sum of seismic strength of all stories is adjusted to maintain the ductility within a predefined target value through the iterative procedure (here, the target was 8). Therefore, a maximum ductility demand of about eight is obtained in all steps. In addition, the weight index has decreased by 9% at step 10 with respect to step 1. As the weight index represents the total seismic strength of a structure, it may be concluded that the model in step 10 with a comparatively lower seismic strength has remained within the same ductility limits. Hence, an enhancement in the distribution of ductility demand is accompanied by a better seismic performance.

Fig. 6 demonstrates the variation of COV in different steps of the iterative procedure toward an optimum pattern for a 10-story building subjected to the 1940 El Centro Earthquake. It shows how COV decreased from 0.25 for the arbitrary pattern in step 1 to a relatively minimum value of about 0.07 in step 104. It is also important to note that the weight index follows a similar trend as shown in Fig. 6.

To examine the validity and comprehensiveness of these findings, numerous analyses were conducted for shear building models with 5, 10 and 15 stories subjected to the 21 earthquakes described in Section 2. For each model, several different distribution patterns were used as the arbitrary pattern for proportioning the story strengths in step 1 of the analysis. Fig. 7 shows that the weight index decrease approaching almost the same value regardless of the distribution pattern used in step 1.

Fig. 7 shows that the solution converges slowly. The relative strength of only one story is modified in each step. Alternatively, a modified procedure could be used to accelerate the convergence. In the modified method, an appropriate modification is applied to the relative strength of all stories in each step. Fig. 7 shows the efficiency of utilizing the modified method that resulted in the weight index decreasing by 44% in only four steps.

Based on the above analyses it is concluded that:

1. Starting from an arbitrary strength distribution pattern, and adjusting it to minimize the COV of story ductility, a pattern that is associated with a minimum COV could be attained.

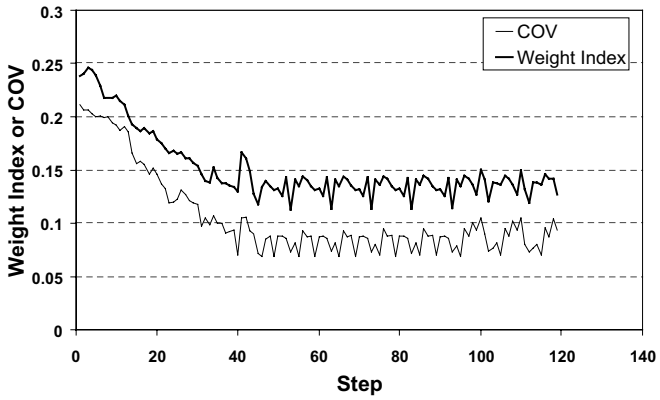

Fig. 6. The correlation between the weight index, *GC* and the coefficient of variation, COV for a 10-story model with period of 0.8 s subjected to El Centro earthquake.

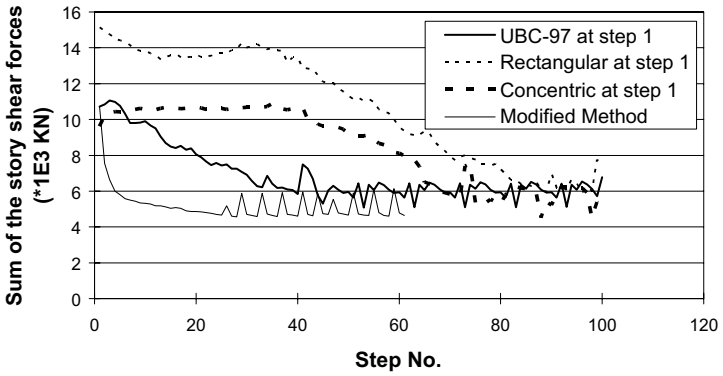

Fig. 7. Variation of total shear strength in the models.

2. The selection of the initial pattern does not affect the results, and eventually in all cases, almost one identical pattern is obtained at the minimal COV points. However, the number of steps required to reach the minimum COV could differ.
3. The weight index always follows a trend similar to the ductility COV, and the two minimize simultaneously. Therefore, it can be concluded that for any given earthquake there is a pattern that leads to an almost uniform distribution of ductility demands with a lower strength.
4. The optimum pattern depends on each earthquake, and varies from one earthquake to another. Hence, the design earthquakes must be classified for each structural performance category and then the best loading pattern must be found by averaging optimum patterns corresponding to every one of the earthquakes in each group. A single loading pattern then could be used for all earthquakes in this group. This method will be explained in the following section.

7. Optimum patterns for prescribed ductility distribution

The design of some buildings requires that different maximum ductility ratios are prescribed for different stories, because of the existence of special conditions in some stories. Therefore, a uniform ductility distribution is not allowed. In these cases, the optimum strength distribution pattern should be the pattern that induces the prescribed distribution in the structure subjected to the given earthquake.

A modified version of the procedure described in the previous section is utilized for this purpose. Fig. 8a shows the variation of the weight index in different iterations for a 10-story building with a period of 1 s subjected to the 1940 El Centro Earthquake. As shown in Fig. 8a, an adequate distribution pattern could be obtained in only five steps. This pattern results in a ductility distribution pattern close to the prescribed ductility distribution with a 52% decrease in the weight index compared to the initial pattern used in step 1. The obtained ductility distribution for this pattern has been compared with the prescribed ductility distribution in Fig. 8b. It is observed that the obtained ductility distribution satisfies the prescribed constraint without any excessive ductility ratio in any one story.

In order to demonstrate the validity of the proposed design method, time history analyses have been performed for all 21 earthquakes and the corresponding optimum pattern has been found for each one. A specific matching base shear has been obtained for each pattern. By averaging the results for all earthquakes, a unique pattern and the corresponding base shear could be obtained. Fig. 9a shows all optimum patterns as well as the average pattern. The coefficient of variation of the patterns in each story

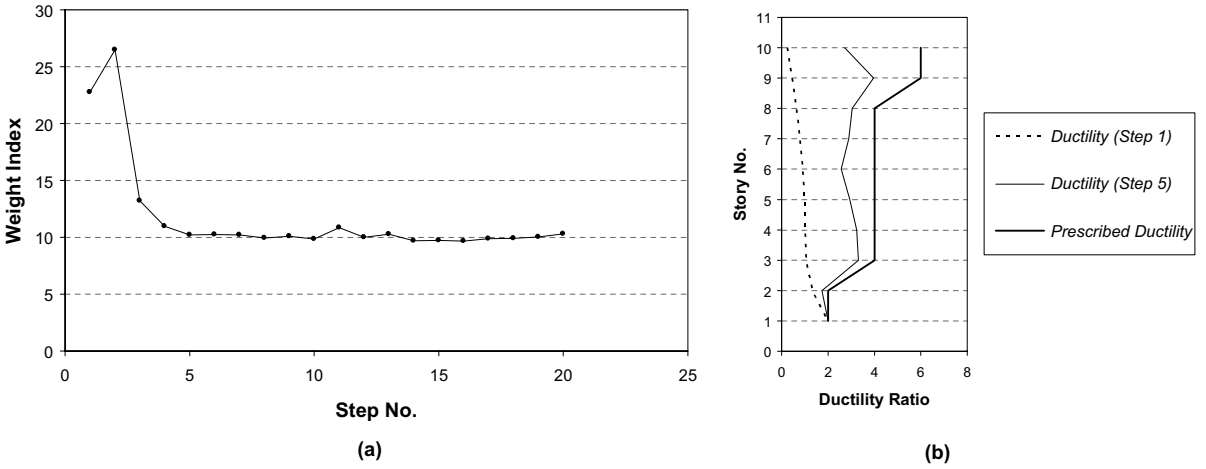

Fig. 8. Design history for 10-story shear building model with a period of 1.0 s subjected to the 1940 El Centro earthquake.

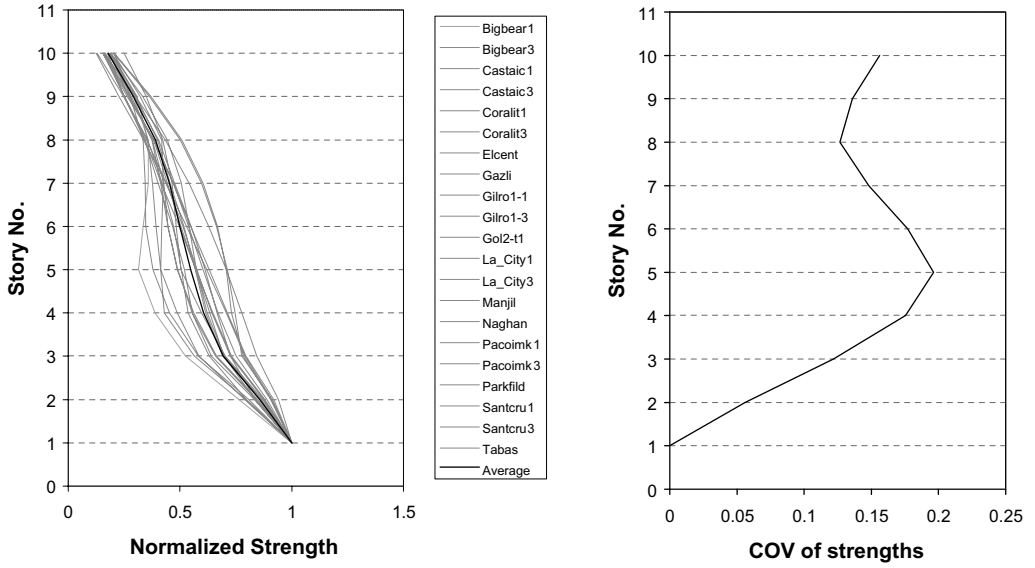

Fig. 9. Average of optimum strength distribution for 10-story shear building model with a period of 1.0 s subjected to 21 earthquake ground motions.

for the 21 earthquakes is shown in Fig. 9b. The average strength pattern and the corresponding base shear were used to design the given 10-story model. Then the response of the designed model to each of the 21 earthquakes was calculated. The average ductility distribution obtained is presented in Fig. 10, which shows that the corresponding ductility distribution is very similar to the prescribed one. It is therefore concluded that the proposed design approach can be used for any ductility distribution and any set of earthquakes, and can provide an efficient performance-based seismic resistant design method for building structures.

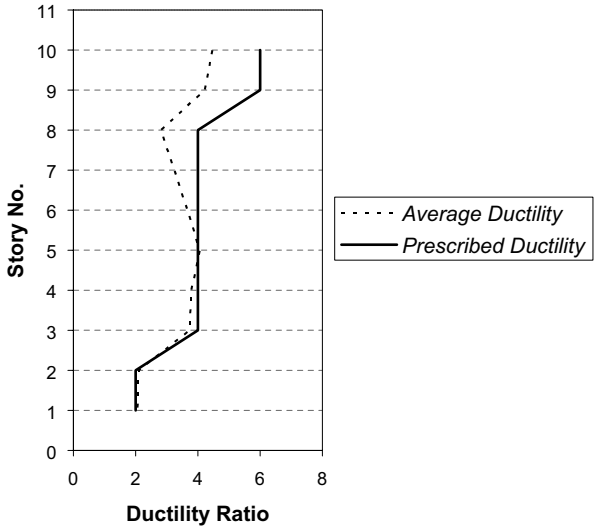

Fig. 10. Average ductility distribution for 10-story shear building model with a period of 1.0 s subjected to 21 earthquake ground motions.

8. Steel frames with viscous dampers

In practical structural design processes of high-rise buildings, a simplified building model such as a shear building model is used for the dynamic response analysis in order to reduce the number of degrees of freedom in the analysis. This simplification is justified if the characteristics of the restoring force in the story level are equivalent in the frame model and its simplified model. Thus, the maximum seismic response of both models is almost equal, even if the building exhibits an elastoplastic response to the earthquake motions (Nakashima et al., 1997; Tsuji and Nakamura, 1996; Takewaki et al., 2000; Uetani et al., 2001). This justification is also valid for buildings with dampers if the stiffness and damping characteristics of the dampers installed in the frame model are transformed appropriately to those for the simplified model.

A building with dampers is usually designed so that the main frame of the building would behave elastically, even if the damper elements display elastoplastic response to design earthquakes. In this case, the equivalence condition between the frame and its simplified model can be expressed by

$$k_i^{\mathrm{S}} = k_i^{\mathrm{F}} \tag{10}$$

where k_i^{S} and k_i^{F} denote the story stiffness of ith story of the simplified model and that of the frame model, respectively. This equivalence condition can also be expressed as follows:

$$\delta_i^{\mathrm{S}} = \delta_i^{\mathrm{F}} \tag{11}$$

where δ_i^{S} and δ_i^{F} denote the interstory drift to horizontal loads of the ith story of the simplified model and the frame model, respectively. If either condition (10) or (11) is satisfied and appropriate stiffness and damping characteristics of dampers are determined, the following equation may be expected to hold:

$$\delta_{i\max}^{\mathrm{S}} \approx \delta_{i\max}^{\mathrm{F}} \tag{12}$$

where $\delta_{i\max}^{\mathrm{S}}$ and $\delta_{i\max}^{\mathrm{F}}$ denote the maximum interstory drift to a design earthquake of the ith story of the simplified model and that of the frame model, respectively. The story stiffness of a frame model depends on the distribution of the horizontal loads.

The design method described in the previous section can be efficiently used to simplified models with passive-type dampers (e.g. shear building models with elastoplastic dampers), such that the distribution of the maximum interstory drifts $\{\delta^{S}_{i\max}\}$ to design earthquakes coincide with the specified set $\{\Delta_i\}$.

The conceptual earthquake resisting mechanism of a structure fitted with elastoplastic dampers, e.g. buckling restrained braces (Kasai et al., 1998) is shown in Fig. 11a. In this figure, the first yielding of the structure corresponds to the yielding of the damper, whereas the yielding of the main frame activates the second yielding. The main key for maximizing the benefit of elastoplastic dampers is to distribute the story drift as uniformly as possible along stories. This is crucial to retard the yielding (damage) to the main frame.

Fig. 11b indicates that the stiffness in the second branch relative to the initial elastic stiffness (referred to hereafter as ratio of second stiffness, β) is a function of the stiffness of the main frame (K_f) and damper (K_d) and is given as $\beta = K_f/(K_f + K_d)$, with the assumption that the damper behaves in an elastic-perfectly plastic manner. Preliminary studies (Karami Mohammadi, 2001) show that β is a key parameter for both the uniformity of distribution of story drift along stories and the control of maximum story drift.

Utilizing the approach proposed in this paper, the optimum distribution of stiffness (and strength) within the structure to achieve a uniform distribution of story drifts could be found for given values of β, number of stories, earthquake ground motion and the viscous damping ratio. Having the optimum stiffness distribution of the simplified model fitted with the dampers, the optimum stiffness distribution of the main frame and dampers can be obtained from the following expressions:

$$K_i = k_{fi} + k_{di} \tag{13a}$$

$$k_{fi} = \beta_i K_i \tag{13b}$$

$$k_{di} = (1 - \beta) K_i \tag{13c}$$

where K_i is the stiffness of the simplified model fitted with the dampers in the ith story. Since β is always less than one, thus dampers' stiffness will always be positive.

While active and passive control systems have received considerable attention, the research on the optimal passive damper placement is limited. Takewaki (1997b), Takewaki et al. (1999), Singh and Moreschi (2001), Diego (2001), Singh and Moreschi (2002), Diego and Soong (2002) and Uetani et al. (2003) investigated the optimum size and location of viscous and viscoelastic dampers within a structure for a given distribution of stiffness. Shear building models have been used in all these studies to find the optimum cases. An innovative optimum design system for structures with passive-type dampers is proposed in Uetani et al. (2003). This design system depends on the type of damper.

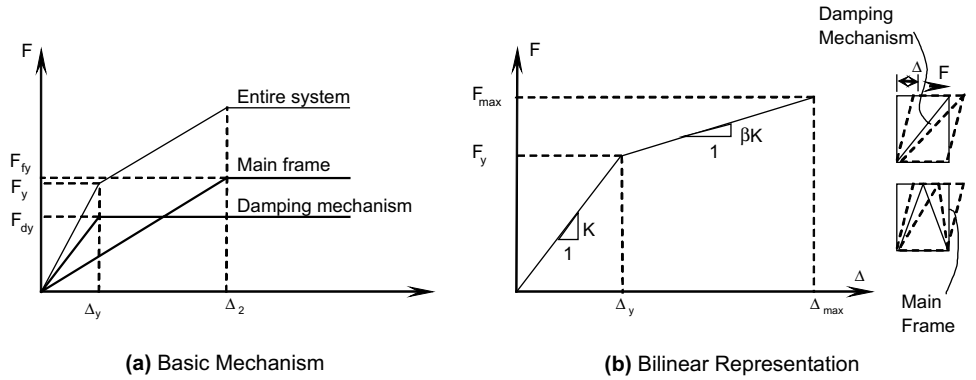

Fig. 11. Conceptual earthquake-resisting mechanism of a structure with hysteretic dampers. (a) Basic mechanism. (b) Bilinear representation.

In the present study, the main objective of optimization problem is the distribution of total stiffness of a structure including the stiffness of the bare frame and hysteretic dampers to achieve a special distribution of structural responses such as story drift (or acceleration). An application example is presented below for practical steel frames with hysteretic dampers.

8.1. Design example

To illustrate the process for designing a structure fitted with elastoplastic dampers, a time-history numerical analysis of a five-story building frame structure with hysteretic dampers subjected to the El Centro Earthquake was performed. In the analysis, the structure was treated as an MDOF spring–mass system, with masses concentrated at the floor level and the story. A bilinear model similar to that shown in Fig. 11b represented the shear versus story deflection relationship. This implies that the main frame was assumed to behave only linearly. Although the real behavior is rather trilinear (Fig. 11a), the analysis adopted the bilinear model because it allows the evaluation of the maximum deflection before the main frame reaches yielding. The mass was divided equally among the stories. The base shear coefficient was set at 0.08, a value smaller than what is normally used, to allow the activation of elastoplastic dampers even under smaller earthquakes. The values of β and the viscous damping ratio used in the analysis were 0.3 and 0.05, respectively. Fig. 12a shows that the story drifts converged to almost the same value in step 10. The story drift distribution in step 10 is shown in Fig. 12b for the optimum stiffness distribution pattern. Having the story stiffnesses of the model fitted with the dampers (K) in this step, the story stiffnesses of the steel frame (K_f) and dampers (K_d) were calculated from Eq. (11) as follows:

$$\underset{(\mathrm{kN/cm})}{K} = \begin{Bmatrix} 4261 \\ 3907 \\ 3343 \\ 2577 \\ 1530 \end{Bmatrix} \Rightarrow K_f = \beta \cdot K = \begin{Bmatrix} 1278 \\ 1172 \\ 1003 \\ 773 \\ 459 \end{Bmatrix} \text{and } K_d = (1-\beta) \cdot K = \begin{Bmatrix} 2983 \\ 2735 \\ 2340 \\ 1804 \\ 1071 \end{Bmatrix} \tag{14}$$

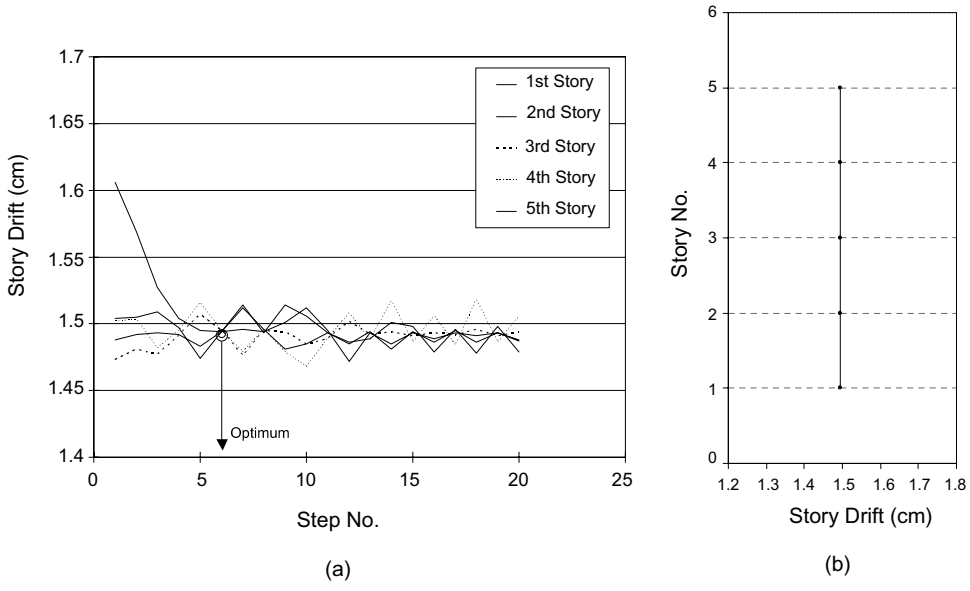

Fig. 12. Analysis results for a five-story model with hysteretic dampers. (a) Variation of story drifts. (b) Story drifts.

A useful result of the buckling restrained brace construction is the ability to independently control strength, stiffness, and yield displacement or ductility by varying the cross-sectional area of the steel core, the yield strength of the steel, and the length of the core allowed to yield (Wada et al., 1992; Clark et al., 2000; Sabelli et al., 2001; Iwata et al., 2000). This provides designers with the opportunity to accurately tailor the force–displacement relationship of their lateral force-resisting elements according to the needs of the application.

9. Conclusions

The control of ductility (and drift) distribution along stories was examined for shear buildings with and without hysteretic dampers. The following conclusions were drawn.

(1) The lateral loading patterns suggested by the seismic codes do not lead to a uniform distribution and minimum ductility demands. A more adequate loading pattern has been proposed. This pattern is a function of the fundamental period of the structure and the target ductility. It was shown that using this pattern could result in a reduction of ductility demands and a more uniform distribution of deformations.
(2) An iterative method to determine the optimum strength distribution pattern for any structure subjected to any given earthquake has been developed. The optimum pattern was found to depend on the earthquake characteristics. Therefore, a single pattern may not be appropriate for all earthquakes and structural characteristics. Catering to the performance-based design approach, a methodology has been introduced to find the best design strength distribution pattern to achieve any desired distribution of ductility (or drift) demands and the least total strength.
(3) Using the proposed design approach, the best stiffness (and strength) distribution within frame structures with hysteretic dampers that could lead to a uniform distribution of story drifts could be obtained for given number of stories, earthquake ground motion, ratio of the second stiffness, and viscous damping ratio.

Acknowledgements

The support of Sharif University of Technology and the Institute for Catastrophic Loss Reduction at the University of Western Ontario are gratefully acknowledged. The authors are grateful to Mr. Iman Hajrasooliha for his computational effort in improving the optimization study.

References

ANSI-ASCE 7-95, 1996. Minimum design loads for building and other structures.

ATC-3-06 Report 1978, Tentative provisions for the development of seismic regulations for buildings. Applied Technology Council, San Francisco, California.

Chopra, A.K., 1995. Dynamics of structures, first ed. Prentice Hall Inc., New Jersey.

Clark, P.W., Kasai, K., Aiken, I.D., Kimura, I., 2000. Evaluation of design methodologies for structures incorporating steel unbonded braces for energy dissipation. In: Proceedings of 12th WCEE, Auckland, New Zealand. Paper No. 2240.

Diaz, O., Mendoza, E., Esteva, L., 1994. Seismic ductility demands predicted by alternate models of building frames. Earthquake Spectra 10 (3), 465–487.

Diego, L.G., 2001. A simple method for the design of optimal damper configurations in MDOF structures. Earthquake Spectra 17 (3), 387–398.

Diego, L.G., Soong, T.T., 2002. Efficiency of a simple approach to damper allocation in MDOF structures. Journal of Structural Control 9 (1), 19–30.

Green, N.B., 1981. Earthquake Resistant Building Design and Construction, second ed. Van Nostrand Reinhold Company, New York.

Iranian Code for Seismic Resistant Design of Buildings, 1999, first ed., Building and Housing Research Center, Tehran.

Iwata, M., Kato, T., Wada, A., 2000. Buckling-restrained braces as hysteretic dampers. In: Behavior of Steel Structures in Seismic Areas (STESSA). Balkema, Rotterdam. pp. 33–38.

Karami Mohammadi, R., 2001. Effects of shear strength distribution on the reduction of seismic damage of structures. D.Phil. thesis. Sharif University of Technology, Tehran, Iran.

Kasai, K., Fu, Y., Watanabe, A., 1998. Passive control systems for seismic damage mitigation. Journal of Structural Engineering, ASCE 124 (5), 501–512.

Lai, M., Li, Y., Zhang, C., 1992. Analysis method of multi-rigid-body model for earthquake responses of shear-type structure. In: Proceedings of 10th WCEE, Madrid, Spain. pp. 4013–4018.

Moghaddam, H., 1996. Earthquake Engineering, first ed., Tehran (in Persian).

Moghaddam, H., Esmailzadeh Hakimi, B., 1999. On the optimum seismic loading of multistory structures. In: Third International Conference on Seismology and Earthquake Engineering, Tehran, Iran. pp. 669–676.

Nakashima, M., Mitani, T., Tsuji, B., 1997. Control of maximum and cumulative deflections in steel building structures combined with hysteretic dampers. Behavior of Steel Structures in Seismic Areas (STESSA). Kyoto, Japan. pp. 744–751.

NEHRP, 1994. Recommended Provisions for the Development of Seismic Regulation for New Buildings. Building Seismic Safety Council, Washington, DC.

Prakash, V., Powell, G.H., Filippou, F.C., 1992. DRAIN-2DX: base program user guide. Report No. UCB/SEMM-92/29. Earthquake Engineering Research Center, University of California, Berkeley.

Sabelli, R., Mahin, S., Chang, C., 2001. Seismic demands on steel braced frame buildings with buckling-restrained braces. In: US–Japan Seminar on Advanced Stability and Seismicity Concept for Performance-Based Design of Steel and Composite Structures, Kyoto, Japan, July 23–26, 2001. pp. 1–20.

Singh, M.P., Moreschi, L.M., 2001. Optimal seismic response control with dampers. Earthquake Engineering and Structural Dynamics 30 (4), 553–572.

Singh, M.P., Moreschi, L.M., 2002. Optimal placement of dampers for passive response control. Earthquake Engineering and Structural Dynamics 31 (4), 955–976.

Takewaki, I., 1996. Design-oriented approximate bound of inelastic responses of a structure under seismic loading. Computers and Structures 61 (3), 431–440.

Takewaki, I., 1997a. Design-oriented ductility bound of a plane frame under seismic loading. Journal of Vibration and Control 3 (4), 411–434.

Takewaki, I., 1997b. Optimal damper placement for minimum transfer functions. Earthquake Engineering and Structural Dynamics 26 (11), 1113–1124.

Takewaki, I., Yoshitomi, S., Uetani, K., Tsuji, M., 1999. Non-monotonic optimal damper placement via steepest direction search. Earthquake Engineering and Structural Dynamics 28 (6), 655–670.

Takewaki, I., Sugimura, Y., Uetani, K., Tsuji, M., Okamoto, T., 2000. Frame design method based on reduced model-frame inverse transformation. In: Proceedings of 12th WCEE, Auckland, New Zealand. Paper No. 1206.

Tsuji, M., Nakamura, T., 1996. Optimum viscous dampers for stiffness design of shear buildings. The Structural Design of Tall Buildings 5, 217–234.

Uetani, K., Tsuji, M., Takewaki, I., 2001. Application of an optimum design method to practical building frames with viscous dampers and hysteretic dampers. In: US–Japan Seminar on Advanced Stability and Seismicity Concept for Performance-Based Design of Steel and Composite Structures, Kyoto, Japan, July 23–26, 2001. pp. 1–12.

Uetani, K., Tsuji, M., Takewaki, I., 2003. Application of an optimum design method to practical building frames with viscous dampers and hysteretic dampers. Engineering Structures 25 (5), 579–592.

Uniform Building Code (UBC) 1997. International Conference of Building Officials.

Wada, A., Connor, J., Kawai, H., Iwata, M., Watanabe, A., 1992. Damage tolerant structure. ATC-15-4 Report. San Diego, California.